ORIGINAL PAPER



A high-pressure Raman study of FeTiO₃ ilmenite: Fermi resonance as a manifestation of Fe-Ti charge transfer

Cara E. Vennari^{1,2} • Quentin Williams³

Received: 18 January 2021 / Accepted: 3 July 2021 © The Author(s), under exclusive licence to Springer-Verlag GmbH Germany, part of Springer Nature 2021

Abstract

We investigated the 300 K high-pressure behavior of ilmenite using Raman spectroscopy to 54 GPa. Upon compression, we observe a Fermi resonance between the lowest frequency A_g symmetry peaks (ν_4 and ν_5) between ~ 10 and ~ 30 GPa: bands that involve major components of Ti–O and Fe–O-related displacements, respectively. The peaks' relative intensities switch at ~ 18 GPa and they also reach their minimum separation at ~ 20 GPa, indicating that their maximum resonance occurs between 18 and 20 GPa. The negative shift of the Ti–O-associated ν_4 vibration under compression is fully consistent with a shift in valence of Ti from 4+ to 3+ under compression. Anomalously small mode shifts of other, more localized vibrations are also consistent with a charge transfer from Fe to Ti under compression. At higher pressures, we have not found definitive evidence for a transition to the perovskite-structure at 300 K, which has been well characterized at high pressures and temperatures. At 40 GPa, we observe an apparent reversible disordering that persists up to our highest pressure. The 300 K mode shifts of the Raman active modes in FeTiO₃ under pressure are notably different from those of other ABO₃ compounds (where A = Mg, Mn and B = Ti, Si); in other ilmenite-structured compounds, the peaks shift at a faster rate and there has not been any observation of Fermi resonance. Thus, iron's complex electronic structure, and its charge transfer with titanium, appears to play a primary role in the behavior of phonons in FeTiO₃ ilmenite.

Keywords Ilmenite · High pressure · Raman spectroscopy · Fermi resonance

Introduction

Ilmenite is a common accessory mineral in igneous and metamorphic rocks on the surface of the Earth. $FeTiO_3$ ilmenite has been of interest for its weak magnetization and its influence on the magnetization of the crust, including remanent magnetization of deeper layers of the crust (Kletetschka et al. 2002). Ilmenite is also an important mineral for understanding the thermo-chemical development of the lunar mantle (Shearer 2006). Additionally, ilmenite has been used as a geological thermometer and redox buffer for igneous and metamorphic rocks (Buddington and Lindsley

1964). From a high-pressure mineral physics perspective, ilmenite is important as a member of the ABX₃ group; the ilmenite structure is adopted by MgSiO₃ at moderate temperatures and deep transition zone pressures, in a range between those of the pyroxene, garnet and perovskite structures (e.g., Ringwood 1970).

The three polymorphs that have been observed in FeTiO₃ are the ilmenite, LiNbO₃ (lithium niobate, LN), and perovskite structures. At high pressures and temperatures, ilmenite has been observed to convert to either LN (Leinenweber et al. 1991) or perovskite (Leinenweber et al. 1995; Ming et al. 2006; Nishio-Hamane et al. 2012). Additionally, the FeTiO₃ LN structure has been observed to transition reversibly to perovskite at 16 GPa at ambient temperature (Leinenweber et al. 1991), and when FeTiO₃ perovskite is decompressed at 300 K, it reverts to the LN structure rather than ilmenite (Ming et al. 2006). At 300 K, one study has shown that ilmenite transitions to perovskite gradually between 20 and 40 GPa (Wu et al. 2009). In contrast, it has been proposed, using density functional theory, that ilmenite will convert to an LN structure at 40 GPa and 0 K

Published online: 01 September 2021



[☐] Cara E. Vennari vennari1@llnl.gov

Department of the Geophysical Sciences, University of Chicago, Chicago, IL, USA

Department of Geology and Geophysics, University of Utah, Salt Lake City, UT, USA

Department of Earth and Planetary Sciences, University of California Santa Cruz, Santa Cruz, CA, USA

(Mehta et al. 1994). Three shock studies have been conducted on FeTiO₃ ilmenite (Simakov et al. 1975; King and Ahrens 1976; Syono et al. 1981). King and Ahrens (1976) observed the onset of anomalous compression at ~30 GPa, while Syono et al. (1981), based on shock recovery experiments, attributed this anomalous behavior to heterogeneous yielding of brittle material. Finally, the oxidation state of Fe has been probed at elevated pressures using Mössbauer and X-ray absorption spectroscopy to understand the degree to which charge transfer occurs from $Fe^{2+} + Ti^{4+}$ to $Fe^{3+} + Ti^{3+}$ under compression (Seda and Hearne 2004; Wu et al. 2009). Although both studies concur that the amount of trivalent iron markedly increases under compression, the absolute amounts differ substantially between these two Mössbauer studies. Seda and Hearne (2004) find that $\sim 40\%$ of the iron is trivalent at 14 GPa (with a particularly rapid shift in the first 2 GPa of compression), while Wu et al. (2009) find a value closer to 15%. This discrepancy was attributed to potential differences between natural and synthetic samples (Wu et al. 2009). From a geophysical/lunar science perspective, one importance of these differing rates is that the electrical conductivity of ilmenite is anticipated to be notably enhanced by this charge-transfer reaction (Seda and Hearne 2004). Accordingly, a possible ilmenite-rich basal layer in the lunar mantle (e.g., Zhang et al. 2017), at pressures near 4 GPa, could influence the propagation of the early lunar magnetic field if the layer is highly conductive.

There have been extensive studies on ilmenite-structured materials with different cations in the A and B sites; we briefly review a few of relevance to our study. A Raman spectroscopic study on MgXO₃ ilmenites, where X = Si, Ge, Ti, was conducted to 30 GPa at 300 K, and no phase changes were observed, nor any soft modes characterized (Okada et al. 2008). LN structured MnTiO₃ converts to perovskite at 300 K at 2 GPa; however, ilmenite-structured MnTiO₂ remained stable to 26.6 GPa (Wu et al. 2011). Additionally, MnTiO3 ilmenite has been shown to convert to the LN structure at high pressures and temperatures (Ko and Prewitt 1988; Ko et al. 1989). In this study, we explore FeTiO₃ at ambient temperature to high pressures using Raman spectroscopy in order to better constrain the phase transformations and charge-transfer transitions of FeTiO3 ilmenite at ambient temperatures.

Methodology

Experiments were conducted on natural ilmenite from Blafjell, Norway with a composition of Fe_{0.98}Mn_{0.07}Ti_{0.94}O₃, as described in King and Ahrens (1976): the sample is a cutting fragment from the same single crystal material on which they performed shock compression experiments. The ambient pressure Raman spectrum is in excellent agreement



Raman measurements were performed using a Horiba LabRAM HR Evolution spectrometer with a 633 nm excitation laser. The spectrometer focal length is 800 mm, and a grating of 1200 lines per millimeter was used with a spectral resolution of ~ 1 cm⁻¹. The laser was focused using an Olympus BXFM-ILHS microscope with a 50×long working distance objective. Spectra were collected from room pressure to 53 GPa at 300 K. Spectra were collected for 20–30 min. Peak positions were calculated from fitting a combination of Gaussian and Lorentzian peaks using the Horiba Labspec6 software.

High pressures were generated using a symmetric diamond anvil cell with type IIa diamonds and 350 m culets. Rhenium was used as the gasket material. The gasket was preindented to ~30 µm and the sample compartment was ~ 150 µm. A pressure medium of 4:1 methanol:ethanol was used. Although this medium is non-hydrostatic above ~ 10 GPa, variable degrees of differential stress typically do not notably affect mode shifts (e.g., Kleppe and Jephcoat 2004; Ruiz-Fuertes et al. 2011; Goryainov 2016; Ott and Williams 2020); such stresses do affect the pressure of, and occasionally occurrence of phase transitions, with phase transitions at times occurring more readily under nonhydrostatic stresses (e.g., Haines and Léger 1997; Sawchuk et al. 2019). The ruby fluorescence technique was used to measure pressure from multiple ruby fragments in the highpressure samples (Dewaele et al. 2008).

Results and discussion

Ambient pressure ilmenite crystalizes in the R-3 space group. The structure consists of a distorted hcp oxygen lattice with two thirds of the cation sites occupied (essentially a corundum structure with alternating Fe and Ti ions). The Fe and Ti are both in octahedral sites and are in alternating layers perpendicular to the c-axis.

Factor group analysis on the ilmenite structure yields 20 normal modes, 10 of which are doubly degenerate, with 10 distinct modes being Raman active:

$$\Gamma = 5A_g(R) + 5E_g(R) + 5A_u(1A + 4IR) + 5E_u(1A + 4IR)$$
(1)

where A designates acoustic modes, IR denotes infrared activity, and R denotes Raman activity.

We observe eight modes at ambient conditions (Fig. 1, Table 1). Since only two symmetry types of Raman modes exist, the spectral modes of ilmenite are often referred to by both their symmetry types and a numerical designation referring to the type of displacement involved in the



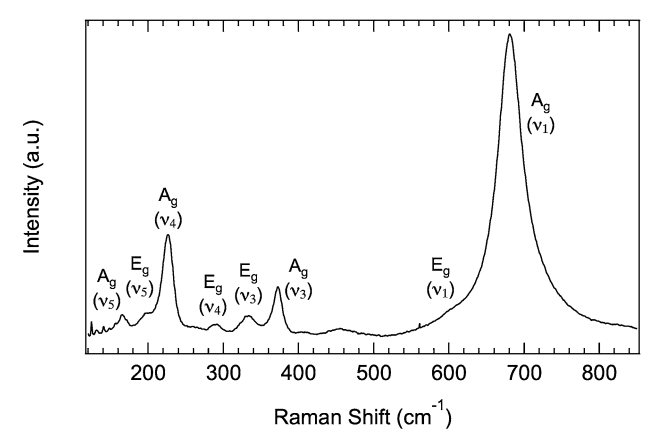


Fig. 1 Ambient pressure and 300 K Raman spectrum of ilmenite

vibration. There is substantial disagreement in the literature over the symmetry assignments (though less so on the atomic motions) of the Raman vibrations of ilmenite. Hofmeister (1993) and Wu et al. (2010) deploy assignments derived from semi-quantitative bond-strength/ reduced mass correlations, while Wang et al. (2008) used polarized Raman spectra and first principles calculations to assign the symmetry species of the spectra. Rodrigues et al. (2018) similarly used lattice dynamics and first principles calculations to assign the symmetry species of the spectra, with results in accord with Wang et al. (2008). Hence, given their combination of both polarized spectra and first principles approaches, we use these latter assignments. The atomic displacements of the Raman active modes are assigned as follows: v_5 vibrations are generally associated with translations of Fe against the oxygen framework, ν_4 can be viewed as predominantly translations of the TiO₆ octahedra against the Fe²⁺ ions, ν_3 and ν_2 are associated with O-Ti-O bends and v_1 are associated with octahedral breathing motions (e.g., Baraton et al. 1994; Wang et al. 2008; Rodrigues et al. 2018). Because both the Fe–O and Ti–O bonds are covalent, the reported assignments represent the dominant atomic motion associated with the vibration; however, it is impossible to fully separate the two octahedral vibrations from each other (Wang et al. 2008; Rodrigues et al. 2018).

The two most intense modes in the ambient Raman spectrum are the $A_o(\nu_4)$, and $A_o(\nu_1)$ modes. Under compression, we are able to track six modes. The three highest frequency Raman active modes $(E_{\sigma}(\nu_3), A_{\sigma}(\nu_3), A_{\sigma}(\nu_1))$ increase close to linearly with frequency up to ~25 GPa; slight deviations from linearity occur above 25-30 GPa (Fig. 2). Two of the lowest frequency modes $(A_{\sigma}(\nu_5), A_{\sigma}(\nu_4))$ interact with each other via a complex resonance that we analyze below, and they do not shift linearly with pressure; neither does the other low-frequency mode, $E_{\sigma}(\nu_5)$. Table 1 summarizes the pressure shifts of each mode. We use high-order polynomials, because the Fermi resonance causes the pressure shifts to deviate significantly from linear or even second-order polynomials. We fit these pressure shifts simply for comparison with the linear pressure shifts of other modes; there is no simple relationship of these fit coefficients (beyond the ambient pressure linear shift) with the thermodynamic parameters of the material, other than that they involve the contributions of single modes to pressure derivatives of the Grüneisen parameter.

Under compression, we observe two major changes to the Raman spectrum with pressure: the first is a change in the low-frequency modes from 10 to 30 GPa which is manifested by intensity changes between the two most intense low-frequency modes and an apparently discontinuous shift in the shoulders on these modes. The second change occurs between 36 and 40 GPa and is characterized by major first-order changes to the Raman spectrum (Fig. 2).

Table 1 Mode assignments, frequencies and pressure shifts of vibrational modes of ilmenite at 300 K; s = strong intensity, m = medium intensity, w = weak intensity, s = strong intensity.

Mode	Assignment	ν_0	Intensity ₀	$d\nu/dP$ (up to ~40 GPa)	\mathbb{R}^2	Mode assign- ment*	MgTiO ₃ (Okada et al. 2008)	MnTiO ₃ (Wu et al. 2011)
$A_g(\nu_5)$ or ν	T(Fe)	165.6	m	$-7E-05P^4+0.0069P^3-0.221P^2+1.926P+$ 224.9	0.9857	$E_g(\nu_5)$	0.966	0.851
$E_g(\nu_5)$	T(Fe)	201.4	w, sh	- 0.116P ² + 1.50P + 209.2 below 15 GPa - 0.0509P ² + 1.7371P + 147.28 above 15 GPa	Below 15 GPa: 0.5393 Above 15 GPa: 0.8458	$\boldsymbol{A}_g(\nu_5)$	1.172	0.953
$A_g(\nu_4)$ or ν_+	$T(TiO_6)$	226.3	S	$0.0012P^3$ - $0.106P^2$ + $2.46P$ + 163.3	0.8969	$E_g(\nu_4)$	1.368	0.898
$E_g(\nu_4)$	$T(TiO_6)$	291.7	W	-		$A_g(\nu_4)$	1.503	1.607
$E_g(\nu_3)$	O-Ti-O bend	333.0	w	2.05(4)		$E_g(\nu_3)$	2.513	2.148
$A_g(\nu_3)$	O-Ti-O bend	371.7	m	2.10(2)		$A_g(\nu_3)$	2.957	2.109
$E_g(\nu_2)$	O-Ti-O bend	-	-	-		$E_g(\nu_2)$	3.218	2.557
$A_g(\nu_2)$	O-Ti-O bend	-	-	-		$A_g(\nu_2)$	4.143	3.132
$E_g(\nu_1)$	Ti-O stretch	608.0	w	-		$E_g(\nu_1)$	4.345	4.371
$A_g(\nu_1)$	Ti-O stretch	681.7	s	1.93(3)		$A_g(\nu_1)$	3.429	2.665

^{*}We provide previous mode assignments from (e.g., Okada et al. 2008) for comparison



34 Page 4 of 9 Physics and Chemistry of Minerals (2021) 48:34

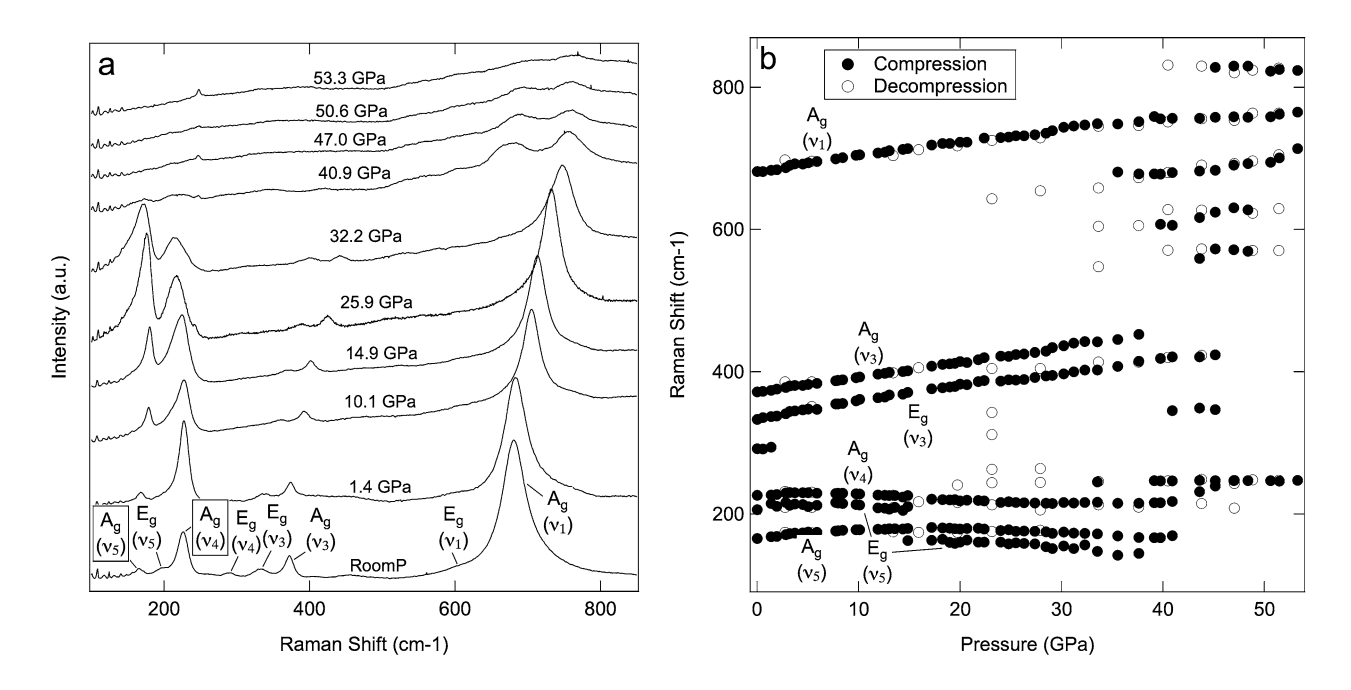


Fig. 2 a Representative Raman spectra of ilmenite under pressure; b peak positions of Raman modes as a function of pressure

Below 40 GPa

The three low-frequency modes that we track initially under pressure consist of two well-defined peaks $(A_o(\nu_5))$ and $A_{\sigma}(\nu_4)$) with a low-frequency shoulder $(E_{\sigma}(\nu_5))$ on the higher frequency $A_{\mathfrak{g}}(\nu_4)$ peak. The three modes do not increase linearly with pressure, and their relative intensities shift dramatically under pressure, with one of the two weaker modes becoming the most intense (Fig. 3a). The higher frequency mode $(A_g(\nu_4))$ and its shoulder $(E_g(\nu_5))$ reach their maximum frequencies at 3.8 GPa and ~230 cm⁻¹ and 6 GPa and ~215 cm⁻¹, respectively. The lower frequency mode (A_{σ}, ν_5) increases, nonlinearly, until 17 GPa and a frequency of ~ 180 cm⁻¹. At ~ 15 GPa, the shoulder $(E_{g}(\nu_{4}))$ on the higher frequency mode, which is manifested as an asymmetry to the low-frequency side of the stronger band, becomes unresolvable, and a new shoulder appears on the lower frequency side of the lower frequency A_o mode $(A_g(\nu_5))$. This shoulder (which may be $E_g(\nu_5)$) continues to lower frequency until it can no longer be observed at 35 GPa. The high-frequency $(A_{\sigma}(\nu_4))$ mode decreases in energy until 30 GPa where it levels out until 40 GPa, while the lower frequency $(A_o(\nu_5))$ mode apparently decreases in energy until the highest pressures probed.

From 0 to 15 GPa, spectral deconvolutions show that the higher frequency $A_g(\nu_4)$ peak decreases in intensity relative to the lower frequency $A_g(\nu_5)$ peak (Fig. 3c). At 16 GPa, their intensities are roughly equal, and from 16 to ~35 GPa, the lower frequency $A_g(\nu_5)$ mode is relatively constant in amplitude, while the higher frequency mode decreases in

strength. At \sim 35 GPa, the spectrum as a whole weakens (Fig. 3a), and the two bands switch their relative intensities again, with the higher frequency mode being more intense until the bands' disappearance at a phase transition.

The three high-frequency modes that steadily increase in frequency are all associated primarily with TiO_6 octahedral vibrations ($E_g(\nu_3)$, $A_g(\nu_3)$, $A_g(\nu_1)$), and they each increase approximately linearly (Table 1) with pressure. We are able to track two O-Ti–O bends with pressure ($E_g(\nu_3)$ and $A_g(\nu_3)$); they both shift at approximately the same rate (Table 1).

Above 40 GPa

At 40 GPa, dramatic changes to the Raman spectrum occur. The lattice modes become largely unresolvable. A new low-frequency mode that remains notably stable in frequency occurs at 30 GPa and ~240 cm⁻¹ and remains until the highest pressure probed. Additionally, four new high-frequency modes appear between 500 and 850 cm⁻¹ to the higher and lower frequency side of the $A_g(\nu_1)$ mode. These new peaks are very broad and low in intensity; their breadth increases and intensities decrease with pressure (Fig. 2), indicating a potentially disordered high-pressure phase. This transition is reversible with hysteresis: upon decompression, the majority of the ilmenite modes return between 20 and 30 GPa.

Fermi resonance

Fermi resonance can occur when two different vibrational modes have the same symmetry (in this case A_g) and have



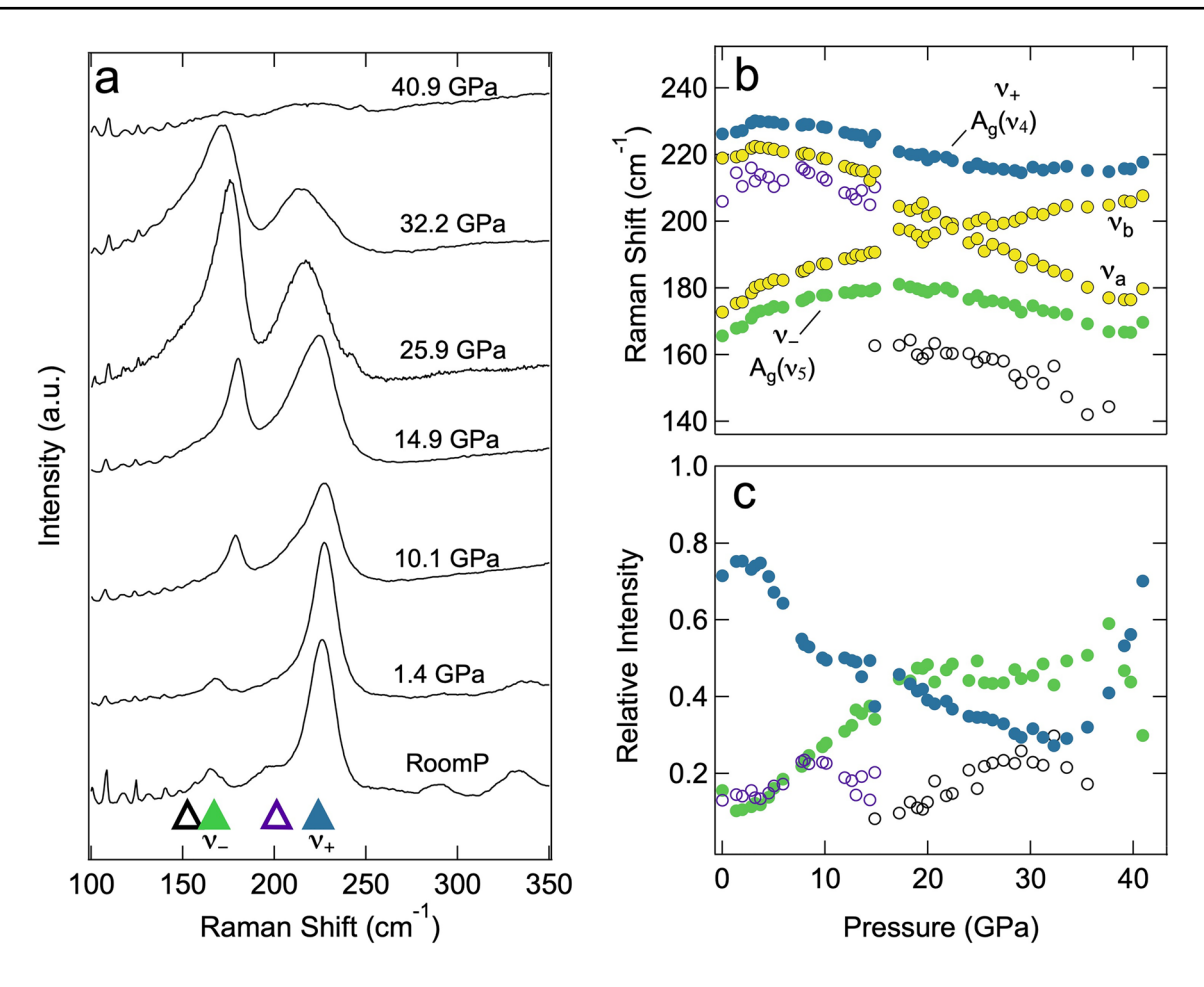


Fig. 3 a Expanded picture of the area of Fermi resonance. Solid triangles represent principal bands, open triangles represent shoulders (the clear asymmetry of the lower frequency peak at high pressures is deconvolved into two peaks), with the colors corresponding to

(b) and (c); b peak positions of Raman modes with pressure (solid), observed modes (open) calculated unperturbed Raman positions; c Relative normalized intensity of the three Raman modes

coincidentally nearly equivalent energies. This similarity in energy leads to a coupling of the two modes, and as the band frequencies approach one another due to shifts in pressure or temperature, the intensity (and, indeed, character) of the bands switch with one another. The bands do not cross, and the maximum resonance can be identified by when the two peaks are at their closest position (in frequency space) and have equivalent intensities. Fermi resonance is most commonly observed between normal modes and overtones (Bier and Jodl 1987; Olijnyk et al. 1988; Knittle et al. 2001; Reed and Williams 2006), however, it has also been observed in materials without the involvement of overtone vibrations (Shimizu 1985; Kawai et al. 1990; Duffy et al. 1995).

Shimizu (1985) described the interaction between two modes, under pressure, undergoing Fermi resonance:

$$(v_+ - v_-)^2 = (v_a - v_b)^2 + 4\delta^2,$$
 (2)

where ν_+ and ν_- are the observed modes, ν_a and ν_b are the unperturbed mode frequencies, and δ is the coupling constant. Using the relation $\nu_+ + \nu_- = \nu_a + \nu_b$, we are able to calculate the frequencies of the modes that are unperturbed by Fermi resonance under pressure (Fig. 3b). The maximum resonance, as determined by the minimum separation (which is also twice the coupling constant) occurs in ilmenite between 18 and 20 GPa and $\delta = 19.8 \text{ cm}^{-1}$.

The precise behavior of the $E_g(\nu_5)$ shoulder is difficult to discern, since its behavior is obscured by the onset of Fermi resonance between the $A_g(\nu_4)$ and $A_g(\nu_5)$ peaks. Its location is derived from the asymmetries to low frequency of the $A_g(\nu_4)$ peak before and after the Fermi resonance (for example, at 10.1 and 25.9 GPa in the spectra of Fig. 3a). It appears that it behaves quite similarly to the $A_g(\nu_4)$ peak, and we note that Rodrigues et al. (2018) document shoulders on peaks in ilmenites that are generated by local deviations from rhombohedral symmetry. We cannot preclude that the shoulder that we monitor and attribute to the weak $E_g(\nu_5)$ peak at high



pressures might not be such a local distortion-induced peak associated with the $A_g(\nu_4)$ peak. The arguments in favor of such an interpretation include that it appears to undergo a comparable Fermi resonance induced shift in apparent frequency near 15 GPa, and that it has a negative shift which is indicative of a predominantly Ti–O-associated vibration, as Ti shifts from tetravalent to trivalent.

The Fermi resonance analysis demonstrates that the Tiassociated $A_{\sigma}(\nu_4, \nu_a)$ vibration is soft, meaning that it has a negative pressure shift (Fig. 3b), while the iron-associated $A_a(\nu_5, \nu_b)$ vibration has a robust positive shift. The negative shift of the $A_{\sigma}(\nu_4, \nu_a)$ mode can be semi-theoretically modeled from a long-standing scaling relation that involves cation-oxygen vibrational frequencies being modeled as scaling as $(Z_1Z_2/\mu d^3)^{1/2}$ (e.g., White and Roy 1964), where Z_1 and Z_2 are the respective charges on the cation and anion, μ is the reduced mass, and d is the interatomic separation. The frequency decrease of the $A_o(\nu_4, \nu_a)$ mode from ~ 220 to ~ 180 cm⁻¹ would, if the vibration is attributed entirely to Ti-O displacements, and there is a shift in charge of Ti from 4 + to 3 +, result in a calculated ratio of the Ti^{3+} -O distance to the Ti⁴⁺-O distance of 1.04. This is in quite good agreement with the ambient pressure ratio of the octahedrallycoordinated Ti³⁺-O/Ti⁴⁺-O distances of 1.033 (Shannon 1976). If charge transfer were incomplete, the agreement between this simple scaling calculation and the observed distance ratio would improve. Similarly, we expect that if no charge transfer occurred under high pressure, the frequencies of each mode would increase with pressure. However, because there is a partial charge transfer at high pressures, the frequency of the vibrations does not solely depend on the compression of the bond lengths; the frequency actually decreases, because Z_1 and Z_2 change with pressure. While recognizing the shortcomings of such a Coulombic harmonic oscillator model, the general agreement here strongly supports the interpretation that the negative shift of the Fermi resonance corrected $A_g(\nu_4)$ mode is generated by the progressive charge-transfer transition of Ti from 4+to 3+over its interval of softening from ~3 to ~40 GPa (Fig. 3b). Because of this softening, the modes approach each other in frequency space, indicating that the Fermi resonance itself is a consequence of the charge transfer and softening of this vibration. Thus, the behavior of this mode reflects the progressive charge transfer across this pressure range.

While no other studies conducted on high-pressure ilmenite-structured compounds have directly characterized a Fermi resonance, Wu et al. (2011), in a Raman study of MnTiO₃ ilmenite, observed substantial intensity changes within the lattice modes (including the modes that we attribute to $A_g(\nu_5)$ and $A_g(\nu_4)$): however, these were not discussed, and might have been generated by changes in crystal orientation as pressure was increased, or within different samples. No notable intensity changes have been

observed in MgTiO₃ ilmenite under pressure (Okada et al. 2008). Also, neither study reported nonlinear peak shifts. The increase in pressure towards the maximum resonance coincides with the pressure-induced charge transfer from Fe²⁺ + Ti⁴⁺ to Fe³⁺ + Ti³⁺ (Seda and Hearne 2004; Wu et al. 2009). These observations indicate that iron's complex and shifting electronic structure relative to that of titanium influences the 300 K stability of Fe-Ti-bearing ilmenite-structured compounds.

Anomalous pressure shifts

The pressure shifts we observe in FeTiO₃ ilmenite are markedly lower than the pressure shift rates reported for MgTiO₃ (Okada et al. 2008) and slightly lower (or equivalent to) pressure shift rates reported for MnTiO₃ (Wu et al. 2011). The most notable difference in the slope of the pressure shift is for the mode associated with the Ti-O stretch $(A_{\alpha}(\nu_1))$. This mode shifts at 1.94(3) cm⁻¹/GPa in FeTiO₃ ilmenite, whereas MgTiO₃ shifts at 3.43 cm⁻¹/GPa and MnTiO₃ shifts at 2.67 cm⁻¹/GPa. We interpret this difference as due to the change in the M²⁺ (Fe²⁺ in this case) cation chemistry. However, this difference is likely primarily associated with the pressure-induced charge transfer from $Fe^{2+} + Ti^{4+}$ to $Fe^{3+} + Ti^{3+}$ as observed by Seda and Hearne (2004) and Wu et al. (2009), and our characterization of a Ti-associated soft mode. Hence, the reduced pressure shifts of the Ti-O stretching mode are directly associated with the shift in valence from Ti⁴⁺ to Ti³⁺. Because the two sets of Fe-O and Ti-O octahedra share oxygens, the frequency of the octahedral stretching vibrations are fundamentally linked to one another. Hence, the charge-transfer must have an even larger effect on the strength of the Fe-O bond to mitigate the pressure-induced changes of the Ti-O bond strength.

This is the effect that is documented in Fig. 4. Here, we compare the linear pressure shifts of three ATiO₃ ilmenite phases at zero pressure, relative to each phase's bulk modulus and cation radius ratio (Fig. 4). For the radius ratio, we use the ambient radius ratio and assume pure A²⁺ and B⁴⁺ in their respective sites. While FeTiO₃ falls only modestly off the trendline between the Mg and Mn end members with respect to both bulk modulus and radius ratio for the O-Ti-O bends ($E_{\sigma}(\nu_3)$ and $A_{\sigma}(\nu_3)$), the pressure dependence is markedly depressed for the Ti-O stretching vibration $(A_{g}(\nu_{1}))$. The pressure shift of this vibration is quite low compared to the Mg and Mn endmembers, and we attribute this markedly lower pressure shift, as with the pressure-induced Fermi resonance, to the charge transfer that occurs under compression and hence the anomalous change in bonding environment associated with the iron and titanium polyhedra.



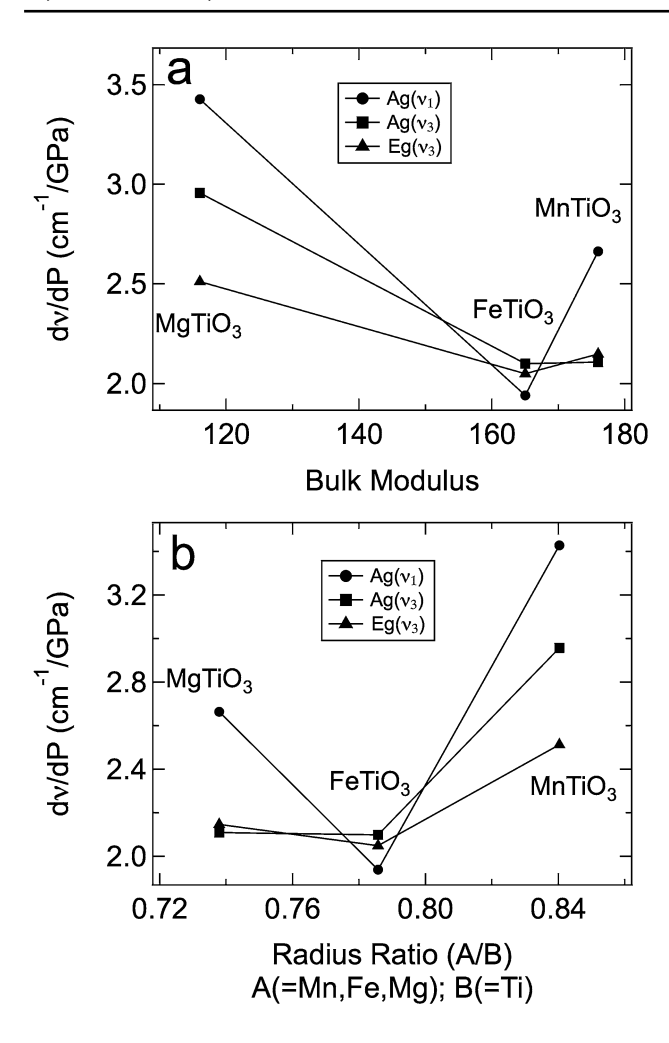


Fig. 4 Comparison of the pressure shifts of Raman modes in three ilmenites compared to (a) bulk modulus and b zero pressure radius ratio. Bulk modulus value for $MgTiO_3$ is from Yamanaka et al. (2005), FeTiO₃ is from Wechsler and Prewitt (1984), and $MnTiO_3$ is from Wu et al. (2011). Pressure shift values for $MgTiO_3$ are from Okada et al. (2008), FeTiO₃ are from this study, and $MnTiO_3$ are from Wu et al. (2011)

High-pressure phase

Above 40 GPa, the peaks not only shift, but become significantly broader, likely indicating a disordered structure. Two phases that ilmenite-structured phases transform to at high pressures (and temperatures) are the lithium niobate (LN) type structure and the perovskite structure. The LN structure is similar to the ilmenite structure in that both the A and B ions are in sixfold coordination; it is related to the ilmenite structure through a cation exchange transition. The transition to perovskite involves a change in coordination number from 6- to 8–12 (hinging on the degree of distortion) for the A ion in the orthorhombic crystal structure and the transition has a displacive character. While the conversion between LN and perovskite may occur readily, the activation energy for a

transition from the ilmenite structure to the LN structure has long been viewed as too large to occur at room temperature (Megaw 1968; Yusa et al. 2006).

Previous studies have observed that ilmenite transforms to perovskite at high pressures and temperatures (Syono et al. 1981; Ming et al. 2006) using shock and static experiments; both of these studies extrapolated the high-temperature transition to 300 K (and arrived at pressures of ~23 and 16 GPa, respectively). Additionally, ilmenite has also been shown to transform to the LN structure at high pressures and temperatures (e.g., Leinenweber et al. 1991; Wu et al. 2011). At 300 K, other ilmenite phases have not been observed to transition to LN or perovskite at 300 K. For example, MgSiO₃, MgTiO₃ and MgGeO₃ are all stable at 300 K up to ~ 30 GPa (Okada et al. 2008). Interestingly, ilmenite-structured MnTiO₃ is stable up to at least ~ 27 GPa, but the LN structured MnTiO₃ transitions to perovskite at 2 GPa (Wu et al. 2011). One study provided evidence for an initiation of the transition of FeTiO₃ ilmenite to perovskite at 20 GPa using Mössbauer spectroscopy, with the transition spanning to~40 GPa (Wu et al. 2009).

Overall, we do not see direct evidence that indicates that the 40 GPa phase is fully crystalline due to its general lack of low-frequency modes and broad high-frequency modes. If the high-pressure phase is LN structured, we would expect more modes, including at lower frequency, as occurs in the MnTiO₃ Raman spectrum (Ko et al. 1989). Similarly, if ilmenite converted to orthorhombic perovskite at high pressure, we would expect many more modes than we observe at 40 GPa. Factor group analysis on GdFeO₃-type (orthorhombic) perovskite yields 24 Raman active modes; nevertheless, ideal cubic perovskite has no first-order active Raman modes and, when present, its observed spectrum is second order (e.g., Williams et al. 1987). McMillan and Ross (1988) provide Raman spectra from perovskites that vary from cubic to varying degrees of orthorhombic distortion via polyhedral tilting; none of these spectra appear similar to that of our observed high-pressure phase. Nevertheless, it is possible that any incipient perovskite phase may have a markedly weak Raman spectrum, and our spectra to 40 GPa may, because of the weak scattering of near-cubic perovskites, only reflect possible residual ilmenite-structured phase within our samples. This interpretation is consistent with that of Wu et al. (2009). Notably, the high-temperature stability field of the perovskite phase appears quite narrow, spanning only 20–30 GPa (Nishio-Hamane et al. 2012), with disproportionation of FeTiO3 to TiO2 and iron-enriched phases at higher pressures.

It is hence possible that our high-pressure spectra may have effectively bypassed the perovskite-structured phase, and accessed a metastable or disordered form of FeTiO₃ at our highest pressure conditions. Given a general similarity between the high-frequency modes in the Raman spectrum



of LN from Ko et al. (1989) and those at the highest pressures in Fig. 2 (two broad, moderately intense high-lying peaks), we suspect that FeTiO₃ may be metastably transforming towards the LN structure. However, the breadth of the peaks and their progressive weakening with increasing pressure indicates that this transition has not gone to completion, and FeTiO₃ may be accessing progressively more disordered states as pressure increases. Perhaps the most compelling evidence that the final state of our samples is not in the perovskite structure is that 300 K decompression of perovskite-structured FeTiO₃ results in a transformation into the LN structure, not ilmenite (e.g., Ming et al. 2006). Because the transition we observe is fully reversible to the ilmenite structure on decompression, it is unlikely that the high-pressure phase that occurs above 40 GPa is perovskite structured.

Conclusions

We have used Raman spectroscopy to probe FeTiO $_3$ ilmenite to 53 GPa. Under compression, we observe a Fermi resonance between a predominantly Fe–O-associated vibration and a soft Ti–O-associated vibration up to 40 GPa, with the maximum resonance between 17 and 20 GPa. Therefore, Raman spectroscopy shows a clear and diagnostic signature of the charge transfer in FeTiO $_3$ ilmenite under compression: this spectroscopic anomaly is not present in any other ilmenite probed to date under compression. At 40 GPa, ilmenite converts to a disordered structure, which may have affinities with either the lithium niobate (LN) or perovskite structure. Given that perovskite reverts to LN between 14 and 16 GPa on decompression, and our highest-pressure phase reverts back to ilmenite at ~30 GPa, we believe this incomplete transition is to either a disordered structure or the LN structure.

Acknowledgements CV acknowledges National Science Foundation (NSF)-EAR-1855336 and QW NSF-EAR-1620423 and EAR-2017294. A portion of this work was performed under the auspices of the US Department of Energy by Lawrence Livermore National Laboratory under Contract No. DE-AC52-07NA27344. We thank two reviewers for helpful and constructive comments. QW is grateful to the late T.J. Ahrens for generously providing the ilmenite sample.

References

- Baraton MI, Busca G, Perito MC et al (1994) Vibrational spectra and structure of NiTiO₃. J Solid State Chem 112:9–14
- Bier KD, Jodl HJ (1987) Tuning of the Fermi resonance of CO₂ and CS₂ by temperature, pressure, and matrix material. J Chem Phys 86:4406–4410. https://doi.org/10.1063/1.452711
- Buddington AF, Lindsley DH (1964) Iron-titanium oxide minerals and synthetic equivalents. J Petrol 5:310–357
- Dewaele A, Torrent M, Loubeyre P, Mezouar M (2008) Compression curves of transition metals in the Mbar range: Experiments and

- projector augmented-wave calculations. Phys Rev B 78:1–13. https://doi.org/10.1103/PhysRevB.78.104102
- Duffy TS, Meade C, Fei Y et al (1995) High-pressure phase transition in brucite, Mg(OH)₂. Am Mineral 80:222–230
- Goryainov SV (2016) Raman study of thaumasite Ca₃Si(OH)₆(SO₄) (CO₃)·12H₂O at high pressure. J Raman Spectrosc 47:984–992. https://doi.org/10.1002/jrs.4936
- Haines J, Léger J (1997) X-ray diffraction study of the phase transitions and structural evolution of tin dioxide at high pressure: Relationships between structure types and implications for other rutile-type dioxides. Phys Rev B Condens Matter Mater Phys 55:11144–11154. https://doi.org/10.1103/PhysRevB.55.11144
- Hofmeister AM (1993) IR reflectance spectra of natural ilmenite: comparison with isostructural compounds and calculation of thermodynamic properties. Eur J Mineral 5:281–296. https://doi.org/10.1127/ejm/5/2/0281
- Kawai NT, Gilson DFR, Butler IS (1990) Variable-temperature and -pressure spectroscopic studies of norbornadiene. J Phys Chem 94:5729–5734. https://doi.org/10.1021/j100378a024
- King DA, Ahrens TJ (1976) Shock compression of ilmenite. J Geophys Res 81:931–935. https://doi.org/10.1029/jb081i005p00931
- Kleppe AK, Jephcoat AP (2004) High-pressure Raman spectroscopic studies of FeS₂ pyrite. Mineral Mag 68:433–441. https://doi.org/10.1180/0026461046830196
- Kletetschka G, Wasilewski PJ, Taylor PT (2002) The role of hematite-ilmenite solid solution in the production of magnetic anomalies in ground- and satellite-based data. Tectonophysics 347:167–177. https://doi.org/10.1016/S0040-1951(01)00243-8
- Knittle E, Phillips W, Williams Q (2001) An infrared and Raman spectroscopic study of gypsum at high pressures. Phys Chem Miner 28(9):630–640
- Ko J, Prewitt CT (1988) High-pressure phase transition in MnTiO₃ from the ilmenite to the LiNbO₃ structure. Phys Chem Miner 15:355–362. https://doi.org/10.1007/BF00311040
- Ko J, Brown NE, Navrotsky A et al (1989) Phase equilibrium and calorimetric study of the transition of MnTiO₃ from the ilmenite to the lithium niobate structure and implications for the stability field of perovskite. Phys Chem Miner 16:727–733. https://doi.org/10.1007/BF00209693
- Lafuente B, Downs RT, Yang H, Stone N (2016) The power of databases: The RRUFF project. In: Highlights in Mineralogical Crystallography. Walter de Gruyter GmbH, pp 1–29
- Leinenweber K, Utsumi W, Tsuchida Y et al (1991) Unquenchable high-pressure perovskite polymorphs of MnSnO₃ and FeTiO₃. Phys Chem Miner 18:244–250
- Leinenweber K, Navrotsky A, Fei Y, Parise JB (1995) High-pressure perovskites on the join CaTiO₃-FeTiO₃. Phys Chem Miner 22:251–258
- McMillan P, Ross N (1988) The Raman spectra of several orthorhombic calcium oxide perovskites. Phys Chem Miner 16:21–28
- Megaw HD (1968) A note on the structure of lithium niobate, LiNbO₃. Acta Crystallogr Sect A 24:583–588. https://doi.org/ 10.1107/S0567739468001282
- Mehta A, Leinenweber K, Navrotsky A, Akaogi M (1994) Calorimetric study of high pressure polymorphism in FeTiO₃: stability of the perovskite phase. Phys Chem Miner 21:207–212. https://doi.org/10.1007/BF00202133
- Ming LC, Kim YH, Uchida T et al (2006) In situ X-ray diffraction study of phase transitions of FeTiO₃ at high pressures and temperatures using a large-volume press and synchrotron radiation. Am Mineral 91:120–126. https://doi.org/10.2138/am.2006.1930
- Nishio-Hamane D, Zhang M, Yagi T, Ma Y (2012) High-pressure and high-temperature phase transitions in FeTiO₃ and a new dense FeTi₃O₇ structure. Am Mineral 97:568–572. https://doi.org/10.2138/am.2012.3973



- Okada T, Narita T, Nagai T, Yamanaka T (2008) Comparative Raman spectroscopic study on ilmenite-type MgSiO₃ (akimotoite), MgGeO₃, and MgTiO₃ (geikielite) at high temperatures and high pressures. Am Mineral 93:39–47. https://doi.org/10.2138/am. 2008.2490
- Olijnyk H, Däufer H, Jodl H-J, Hochheimer HD (1988) Effect of pressure and temperature on the Raman spectra of solid CO₂. J Chem Phys 88:4204–4212. https://doi.org/10.1063/1.453828
- Ott JN, Williams Q (2020) Raman spectroscopic constraints on compression and metastability of the amphibole tremolite at high pressures and temperatures. Phys Chem Miner 47:1–13. https://doi.org/10.1007/s00269-020-01095-6
- Reed JW, Williams Q (2006) An infrared spectroscopic study of NH₄Br-ammonium bromide to 55 GPa. Solid State Commun 140:202–207. https://doi.org/10.1016/j.ssc.2006.07.036
- Ringwood AE (1970) Phase transformations and the constitution of the mantle. Phys Earth Planet Inter 3:109–155. https://doi.org/10.1016/0031-9201(70)90047-6
- Rodrigues JE, Ferrer MM, Cunha TR et al (2018) First-principles calculations and Raman scattering evidence for local symmetry lowering in rhombohedral ilmenite: temperature- and pressure-dependent studies. J Phys Condens Matter. https://doi.org/10.1088/1361-648X/aae803
- Ruiz-Fuertes J, Errandonea D, López-Moreno S et al (2011) High-pressure Raman spectroscopy and lattice-dynamics calculations on scintillating MgWO₄: comparison with isomorphic compounds. Phys Rev B Condens Matter Mater Phys 83:1–11. https://doi.org/10.1103/PhysRevB.83.214112
- Sawchuk K, O'Bannon EF, Vennari C et al (2019) An infrared and Raman spectroscopic study of PbSO₄-anglesite at high pressures. Phys Chem Miner 46:623–637. https://doi.org/10.1007/s00269-019-01027-z
- Seda T, Hearne GR (2004) Pressure induced $Fe^{2+} + Ti^{4+} \rightarrow Fe^{3+} + Ti^{3+}$ intervalence charge transfer and the Fe^{3+}/Fe^{2+} ratio in natural ilmenite (FeTiO₃) minerals. J Phys Condens Matter 16:2707–2718. https://doi.org/10.1088/0953-8984/16/15/021
- Shannon RD (1976) Revised effective ionic radii and systematic studies of interatomic distances in halides and chalcogenides. Acta Crystallogr Sect A 32:751–767. https://doi.org/10.1107/S0567739476001551
- Shearer CK (2006) Thermal and magmatic evolution of the Moon. Rev Mineral Geochem 60:365–518. https://doi.org/10.2138/rmg. 2006 60 4
- Shimizu H (1985) Pressure-tuning resonance between the vibron and the libron in CH_2Br_2 and CD_2Br_2 molecular solids. Phys Rev B 32:4120–4125

- Simakov G, Pavlovskii M, Kalashnikov N, Trunin R (1975) Shock compressibility of twelve minerals. Izv Acad Sci USSR Phys Solid Earth 8:488–492
- Syono Y, Takei H, Goto T, Ito A (1981) Single crystal X-ray and Mössbauer study of shocked ilmenite to 80 GPa. Phys Chem Miner 7:82–87. https://doi.org/10.1007/BF00309456
- Wang CH, Jing XP, Feng W, Lu J (2008) Assignment of Raman-active vibrational modes of MgTiO₃. J Appl Phys. https://doi.org/10. 1063/1.2966717
- Wechsler BA, Prewitt CT (1984) Crystal structure of ilmenite (FeTiO₃) at high temperature and at high pressure. Am Mineral 69:176–185
- Williams Q, Jeanloz R, McMillan P (1987) Vibrational spectrum of MgSiO₃ perovskite: zero-pressure Raman and mid-infrared spectra to 27 GPa. J Geophys Res 92:8116–8128. https://doi.org/10.1029/JB092iB11p11670
- Wu X, Steinle-Neumann G, Narygina O et al (2009) Iron oxidation state of FeTiO₃ under high pressure. Phys Rev B - Condens Matter Mater Phys 79:1–7. https://doi.org/10.1103/PhysRevB.79.094106
- Wu X, Qin S, Dubrovinsky L (2010) Structural characterization of the FeTiO₃-MnTiO₃ solid solution. J Solid State Chem 183:2483–2489. https://doi.org/10.1016/j.jssc.2010.08.020
- Wu X, Qin S, Dubrovinsky L (2011) Investigation into high-pressure behavior of MnTiO₃: X-ray diffraction and Raman spectroscopy with diamond anvil cells. Geosci Front 2:107–114. https://doi.org/ 10.1016/j.gsf.2010.09.003
- Yamanaka T, Komatsu Y, Sugahara M, Nagai T (2005) Structure change of MgSiO₃, MgGeO₃, and MgTiO₃ ilmenites under compression. Am Mineral 90:1301–1307. https://doi.org/10.2138/am. 2005.1621
- Yusa H, Akaogi M, Sata N et al (2006) High-pressure transformations of ilmenite to perovskite, and lithium niobate to perovskite in zinc germanate. Phys Chem Miner 33:217–226. https://doi.org/ 10.1007/s00269-006-0070-5
- Zhang N, Dygert N, Liang Y, Parmentier EM (2017) The effect of ilmenite viscosity on the dynamics and evolution of an overturned lunar cumulate mantle. Geophys Res Lett 44:6543–6552. https://doi.org/10.1002/2017GL073702

Publisher's Note Springer Nature remains neutral with regard to jurisdictional claims in published maps and institutional affiliations.

